Int. J. Solids Structures, 1976, Vol. 12, pp. 13–26. Pergamon Press. Printed in Great Britain

DOUBLE CANTILEVER BEAM MODELS IN ADHESIVE MECHANICS

D. J. CHANG
The Aerospace Corp., El Segundo, CA 90245, U.S.A.

and

R. MUKI and R. A. WESTMANN
Mechanics and Structures Department, School of Engineering and Applied Science,
University of California, Los Angeles, CA 90024, U.S.A.

(*Received* 3 *April* 1974; *revised* 27 *May* 1975)

1. INTRODUCTION

There is a growing need to accurately predict failure of adhesive joints. To meet this, mechanics researchers are turning to fracture mechanics[1]. Application of modern fracture mechanics to adhesive joints depends upon a stress analysis and characterization of the singular stress fields within the connection. In the application of fracture mechanics to crack propagation problems this poses only a moderate problem as there have been significant advances in the stress analysis of crack geometries.

Unfortunately, the geometry associated with an adhesive joint such as a shear lap joint is extremely complicated. The adherends are flexible and the joint rotates, the adhesive layer has a finite thickness and possibly possesses non-linear and rate-dependent mechanical properties, while the adherend thickness may vary. The stress analysis problems are formidable.

Some progress has been made by introducing simplifying assumptions and employing the two-dimensional theory of elasto-statics[2, 3]. On the other hand, numerical methods such as finite elements[4] appear promising and, when properly employed, should prove useful. While both of these approaches are important and valuable, they are also difficult, time consuming and expensive. This difficulty in the stress analysis is proving to be a deterrent to the basic understanding of the physics and phenomena of adhesive joint failure.

An interesting alternative is to use an approximate structural theory in the stress analysis. In this way it might be possible to extract much of the essential information without extensive mathematical or numerical work. In fact, the first stress analyses of adhesive joints[5–7] were done in this spirit although not with a fracture mechanics analysis as the prime goal.

In the case of an adhesive joint joining two slender members, it is particularly appealing to use plate or beam theories to simplify the stress analysis. For example, the use of simple beam theory by Gilman[8] proved quite useful in the understanding of the double cantilever beam test specimen. Subsequently the approximate predictions were refined by numerical and experimental methods[9–12] but the basic results presented in [8] are still valuable. A similar approach based upon a refined plate theory [13] was used in [14] to solve a related problem.

A recent paper by Kanninen[15] has modified Gilman's analysis by approximately accounting for the thickness deformations in the beam. Suitable selection of a somewhat arbitrary parameter in Kanninen's model has led to excellent agreement with established results[9–12]. Kanninen's paper gives a good example of how an approximate structural theory can be successfully employed.

As a long range goal it is desirable to develop an approximate but accurate structural theory for adhesive connections. Such a theory would permit approximate analysis of adhesive joints accounting for the effects of inelasticity, joint geometry, and bond line properties. The accuracy of such a theory must, of course, be assessed whenever possible by comparison with elasticity and experimental results.

This paper is concerned with two alternative models of the double cantilever specimen and comparison of the responses predicted by the two models. In Section 2 we develop a solution to an idealized model of the double cantilever problem, the solution being exact within the framework of the geometric simplifications and the two dimensional elastostatic theory of plane

strain. Particular attention is focused on the asymptotic behavior of the stress intensity factor for certain ranges of the geometric parameters. Section 3 presents a new approximate structural theory for the problem and a solution is obtained permitting evaluation of the bond line tractions including the singular field. In Section 4, numerical results are presented and the "exact" and approximate results are compared with each other and earlier work. It is found that the approximate structural theory employed is quite accurate and yields good results for a wide range of the geometric parameters of interest. Accordingly, it is expected that the model can be extended and employed in the investigation of certain other types of adhesive joints.

2. TWO DIMENSIONAL ELASTICITY MODEL

In this section, certain geometric approximations are made and a solution obtained using the two-dimensional elasticity theory of plane strain. The cross section of an actual double cantilever specimen (DCB) is shown in Fig. 1a, the bonded portion represented by the dotted line.

To facilitate the analysis let the upper and the lower plates be infinite in extent and bounded by two parallel planes separated by a distance h (plate thickness), each plate possessing the same homogeneous and isotropic elastic properties. A cartesian coordinate system is chosen with the x–y plane located in the undeformed middle plane of the upper plate as shown in Fig. 1b. The displacements and stresses of interest in the plates are denoted by u, w and σ_{xx}, σ_{zz}, τ_{xz}, respectively.

Now let the two plates be bonded together along the interface $z = -h/2$, $-a < x < 0$. It is assumed that the bond line is sufficiently thin so that we can neglect its thickness and properties. The loading consists of two opposing concentrated cleavage forces applied at points $x = l$ as shown in Fig. 1b.

The greatest error in this geometric approximation of the DCB is the neglect of the traction free back face at $x = -a$, $-(3/2)h < z < h/2$. Intuitively, it is felt that this should not be significant provided $a/h > 3$.

The symmetry of the geometry and loading leads to the following boundary conditions for the upper plate:

$$\left.\begin{aligned} &\sigma_{zz}(x, h/2) = \tau_{xz}(x, h/2) = 0 && (-\infty < x < \infty), \\ &\sigma_{zz}(x, -h/2) = -P_0\delta(x-l), \quad \tau_{xz}(x, -h/2) = 0 && (-\infty < x < -a,\ 0 < x < \infty), \\ &\tau_{xz}(x, -h/2) = 0, \quad \left.\frac{\partial w}{\partial z}\right|_{z=-h/2} = 0 && (-a < x < 0), \end{aligned}\right\} \tag{1}$$

where $\delta(\ )$ is the Dirac delta function. Also, it is necessary to impose the regularity requirement

$$\sigma_{xx}, \sigma_{zz}, \tau_{xz} \to 0 \qquad \text{as } |x| \to \infty. \tag{2}$$

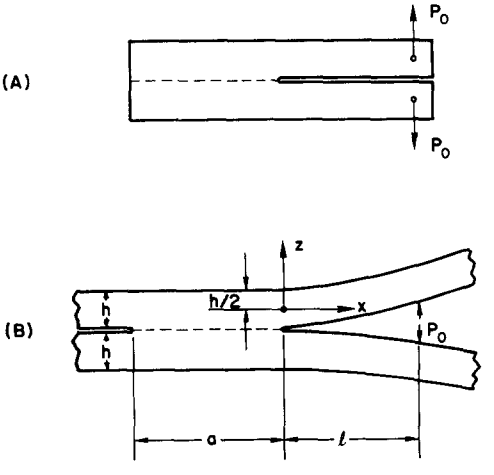

Fig. 1. Geometry of double cantilever.

In view of the overall equilibrium requirements for the upper plate, $\sigma_{zz}(x, -h/2)$ over the bonded region must satisfy the constraint conditions

$$\int_{-a}^{0} \sigma_{zz}(x, -h/2)\,dx - P_0 = 0, \quad \int_{-a}^{0} x\sigma_{zz}(x, -h/2)\,dx - lP_0 = 0. \tag{3}$$

To proceed with the solution, it is first convenient to introduce an auxiliary stress field $\mathring{\sigma}_{xx}$, $\mathring{\sigma}_{zz}$, $\mathring{\tau}_{xz}$ subject to the boundary conditions

$$\left.\begin{aligned} &\mathring{\sigma}_{zz}(x, h/2) = \mathring{\tau}_{xz}(x, h/2) = 0, \\ &\mathring{\sigma}_{zz}(x, -h/2) = -\delta(x), \quad \mathring{\tau}_{xz}(x, -h/2) = 0 \ (-\infty < x < \infty), \end{aligned}\right\} \tag{4}$$

and the regularity requirements

$$\begin{aligned} &\mathring{\sigma}_{xx}, \mathring{\sigma}_{zz}, \mathring{\tau}_{xz} = 0(|x|^{\lambda}) \qquad \text{as } x \to -\infty, \\ &\mathring{\sigma}_{xx}, \mathring{\sigma}_{zz}, \mathring{\tau}_{xz} = 0(e^{-\epsilon x}) \qquad \text{as } x \to \infty, \end{aligned} \tag{5}$$

that are uniformly valid on $-h/2 \le z \le h/2$ for some positive λ and ϵ.

Routine calculations using Airy's stress function and the exponential Fourier transform lead to integral representations for the stresses, see [3]†. From these integral representations of the stresses and by use of a residue calculation the following asymptotic behavior is determined:

$$\left.\begin{aligned} \mathring{\sigma}_{xx}(x, z) = &\begin{cases} \dfrac{12xz}{h^2} + 0\,(e^{-(\pi|x|)/h}) & \text{as } x \to -\infty, \\ 0(e^{-(\pi x/h)}) & \text{as } x \to \infty, \end{cases} \\ \mathring{\sigma}_{zz}(x, z) = &\ 0(e^{-(\pi|x|)/h}) \qquad \text{as } |x| \to \infty, \\ \mathring{\tau}_{xz}(x, z) = &\begin{cases} \dfrac{3}{2h}\left(1 - \dfrac{4z^2}{h^2}\right) + 0(e^{-(\pi|x|)/h}) & \text{as } x \to -\infty, \\ 0\,(e^{-(\pi x/h)}) & \text{as } x \to \infty. \end{cases} \end{aligned}\right\} \tag{6}$$

thereby satisfying regularity requirements (5).

Let $\mathring{u}$, $\mathring{w}$ be the displacements associated with $\mathring{\sigma}_{xx}$, $\mathring{\sigma}_{zz}$, $\mathring{\tau}_{xz}$. A key item in subsequent calculations is the derivative of $\mathring{w}$ with respect to x along the lower edge. This is obtained from the integral representations of the stress field and has the form

$$\left.\frac{\partial \mathring{w}}{\partial x}\right|_{z=-h/2} = \theta(x) = \frac{2(1-\nu^2)}{\pi h E}\left[-\frac{h}{x} + F\left(\frac{x}{h}\right)\right] \ (0 < |x| < \infty), \tag{7}$$‡

where E, ν are Young's modulus and Poisson's ratio respectively, while

$$\left.\begin{aligned} F(\xi) &= -\frac{3\pi}{2}\xi^2 + \frac{3\pi}{5} + \int_0^{\infty}\left[f(s)\sin(\xi s) + \frac{6\xi}{s^2}\right]ds, \\ f(s) &= \frac{s + 1 - e^{-s}}{2[\sinh(s) + s]} - \frac{s + 1 + e^{-s}}{2[\sinh(s) - s]}. \end{aligned}\right\} \tag{8}$$

To find the behavior of $\partial \mathring{w}/\partial x|_{z=-h/2}$ as x goes to infinity, decompose F as indicated below,

†In [3], notations x_1, x_2, b are used for $x, z, h/2$ here and stresses $\tau_{11}^{(1)}, \tau_{22}^{(1)}, \tau_{12}^{(1)}$ correspond to $\mathring{\sigma}_{xx}, \mathring{\sigma}_{zz}, \mathring{\tau}_{xz}$ here. See (3) in [3].

‡See [3] for a derivation of this result.

$\left.\dfrac{\partial \mathring{w}}{\partial x}\right|_{z=-h/2}$ here corresponds to $\dfrac{\partial u_2}{\partial x_1}(x_1, -b)$ in [3]. See (5) in [3].

integrate the first explicitly and apply the Riemann-Lebesgue lemma to the second integral. Then it results that

$$F(\xi)=\frac{3\pi}{2}\xi^2+\frac{3\pi}{5}-6\int_0^\infty\left[\left(\frac{1}{s^3}+\frac{1}{5s}\right)\sin(\xi s)-\frac{\xi}{s^2}\right]ds$$
$$+\int_0^\infty\left[f(s)+6\left(\frac{1}{s^3}+\frac{1}{5s}\right)\right]\sin(\xi s)\,ds$$
$$=\begin{cases}o(1) & \text{as } \xi\to\infty,\\ -3\pi\xi^2+\dfrac{6\pi}{5}+o(1) & \text{as } \xi\to-\infty.\end{cases}\tag{9}$$

Substituting F from (9) into (7) yields

$$\lim_{x\to\infty}\frac{\partial\mathring{w}}{\partial x}\bigg|_{z=-h/2}=0.\tag{10}$$

Our next objective is to establish an integral equation for the bond stress $\sigma_{zz}(x,-h/2)$ in the interval $(-a,0)$ which we denote by $p(x)$. Once p is determined, stresses in the adhesive joint can easily be evaluated using superposition and our knowledge of the auxiliary stress field $\mathring{\sigma}_{xx}$, $\mathring{\sigma}_{zz}$, $\mathring{\sigma}_{xz}$. For example, we have

$$\sigma_{xx}(x,z)=P_0\mathring{\sigma}_{xx}(x-l,z)-\int_{-a}^{0}p(s)\mathring{\sigma}_{xx}(x-s,z)\,ds$$
$$(-\infty<x<\infty,\ -h/2<z<h/2).\tag{11}$$

Now observe that the last of (1), the bond condition, essentially implies that the bond line remains straight after loading. Accordingly, replace the last of (1) by

$$\frac{\partial w}{\partial x}\bigg|_{z=-h/2}=\omega\qquad(-a<x<0),\tag{12}$$

where ω is the slope of the bond line relative to that of the edge as $x\to\infty$. The actual value of ω is not of particular interest, but must be included in the formulation to permit the satisfaction of the overall equilibrium condition (3). Use of superposition leads to the following restatement of condition (12) in terms of the applied load and bond line stress;

$$P_0\theta(x-l)-\int_{-a}^{0}p(s)\theta(x-s)\,ds=\omega\qquad(-a<x<0).\tag{13}$$

Substitution of θ from (7) into (13) yields the following singular integral equation for p:

$$\int_{-a}^{0}\frac{p(t)}{t-x}\,dt=B+\psi(x)\qquad(-a<x<0),\tag{14}$$

where B is a constant involving ω and

$$\psi(x)=\frac{P_0}{h}\left[F\left(\frac{x-l}{h}\right)+\frac{h}{l-x}\right]-\frac{1}{h}\int_{-a}^{0}p(y)F\left(\frac{x-y}{h}\right)dy.\tag{15}$$

The integral eqn (14) is accompanied by the constraint conditions

$$\int_{-a}^{0}p(t)\,dt=P_0,\qquad\int_{-a}^{0}tp(t)\,dt=P_0l\tag{16}$$

which follow from (3) and the definition of p.

To facilitate the numerical solution we reduce the singular integral equation (14) to a standard Fredholm integral equation by means of Muskhelishvili's method ([16], p. 235). In this manner it is determined from (14) that

$$\left.\begin{aligned} p(t_0) = &-\frac{1}{\pi^2\sqrt{-t_0(t_0+a)}}\int_{-a}^{0}\frac{\sqrt{-t(t+a)}}{t-t_0}[B+\psi(t)]\,dt \\ &+\frac{A}{\sqrt{-t_0(t_0+a)}} \qquad (-a<t_0<0), \end{aligned}\right\} \tag{17}$$

where A and B are undetermined constants.

To determine A, B, substitute from (17) into constraint conditions (16). Completion of the integrations involved then leads to

$$\begin{aligned} A &= \frac{P_0}{\pi}, \\ \frac{a^2B}{8} &= P_0\left(l+\frac{a}{2}\right)-\frac{1}{\pi}\int_{-a}^{0}\sqrt{-t(t+a)}\psi(t)\,dt. \end{aligned} \tag{18}$$

Inspection of the integral eqn (17) together with (15), (18) and the definition of p suggests the introduction of the following dimensionless variables and constants

$$\left.\begin{aligned} &\alpha = a/h, \quad \lambda = l/h, \quad \xi = -t/h, \\ &\phi(\xi) = \sqrt{-x(a+x)}\cdot\frac{\sigma_{zz}(x,-h/2)}{P_0} = h\sqrt{\xi(\alpha-\xi)}\cdot\frac{p(-h\xi)}{P_0}. \end{aligned}\right\} \tag{19}$$

Then, after permissible interchange of the order of integration and use of (18) and (15), the integral equation (17) reduces to

$$\phi(\xi)-\int_0^{\alpha}K(\xi,\eta)\phi(\eta)\,d\eta = H(\xi) \qquad (0\le\xi\le\alpha), \tag{20}$$

where

$$\left.\begin{aligned} K(\xi,\eta) = &\frac{1}{\pi^2\sqrt{\eta(\alpha-\eta)}}\int_0^{\alpha}\sqrt{\zeta(\alpha-\zeta)}\cdot\left[\frac{4}{\alpha}-\frac{8\xi}{\alpha^2}-\frac{1}{\zeta-\xi}\right] \\ &\cdot F(\eta-\zeta)\,d\zeta \qquad (0\le\xi<\alpha,\ 0<\eta<\alpha), \\ H(\xi) = &\frac{1}{\pi}\left[1+\frac{2}{\alpha^2}(\alpha-2\xi)(\alpha+2\lambda)\right] \\ &-\frac{1}{\pi^2}\int_0^{\alpha}\sqrt{\zeta(\alpha-\zeta)}\cdot\left[\frac{4}{\alpha}-\frac{8\xi}{\alpha^2}-\frac{1}{\zeta-\xi}\right] \\ &\cdot\left[\frac{1}{\lambda+\xi}+F(-(\lambda+\zeta))\right]d\zeta \qquad (0\le\xi\le\alpha). \end{aligned}\right\} \tag{21}$$

It can be shown that the solution to (20) is bounded. Therefore, it follows from (19) that the bond line traction, $\sigma_{zz}(x,-h/2)$, has an inverse square root singularity at the ends of the bond line.

The stress intensity factor K_I,[17] describing the singular field at the end of the bond line $x=0$ can be expressed in terms of $\phi(0)$ by the aid of (19) as

$$K_I = \lim_{x\to 0-}\sqrt{-2\pi x}\,\sigma_{zz}(x,-h/2) = P_0\sqrt{\frac{2\pi}{h}}\frac{\phi(0)}{\sqrt{\alpha}}. \tag{22}$$

A dimensionless stress intensity factor κ is defined as

$$\kappa(\alpha, \lambda) = \frac{K_I}{P_0}\sqrt{\frac{h}{2\pi}} = \frac{1}{\sqrt{\alpha}}\phi(0; \alpha, \lambda) \tag{23}$$

where the dependence on the parameters α, λ is now explicitly stated.

To determine the behavior of κ as $\lambda = l/h \to 0$, $\alpha \neq 0$ consider a cleavage problem for the entire plane with a crack along the positive x-axis. This is appropriate since influence of the thickness of the plate and of the length of the bond line "a" upon stresses in the vicinity of the origin disappears in the limit as $l \to 0$. Let $\hat{u}$, $\hat{\omega}$ and $\hat{\sigma}_{xx}$, $\hat{\sigma}_{zz}$, $\hat{\tau}_{xz}$ be the displacements and stresses in the cut plane subject to the boundary conditions

$$\left.\begin{aligned} &\hat{\sigma}_{zz}(x, 0) = -P_0\delta(x - l) && (0 < x < \infty), \\ &\hat{\tau}_{xz}(x, 0) = 0 && (-\infty < x < \infty), \\ &\hat{w}(x, 0) = 0 && (-\infty < x < 0). \end{aligned}\right\} \tag{24}$$

and the regularity requirements

$$\hat{\sigma}_{xx}, \hat{\sigma}_{zz}, \hat{\tau}_{xz} = o(1) \qquad \text{as } x^2 + z^2 \to \infty. \tag{25}$$

The solution to this problem is well known[18] and the bond line stress is given by

$$\hat{\sigma}_{zz}(x, 0) = \frac{P_0}{\pi}\frac{1}{\sqrt{-xl}} + 0(1) \qquad \text{as } x \to 0-. \tag{26}$$

Thus, it follows from (22), (23), (19) and (26) that

$$\kappa(\alpha, \lambda) = \frac{1}{\pi\sqrt{\lambda}} + 0(1) \qquad \text{as } \lambda \to 0. \tag{27}$$

It is also desirable to establish an approximate expression for κ valid for large λ. To accomplish this observe that the kernel $K(\xi, \eta)$ of the integral eqn (20) does not depend on λ. On the other hand, the forcing function $H(\xi)$ does depend upon this parameter. The asymptotic behavior of $H(\xi)$ as $\lambda \to \infty$ is determined by substituting F from (9) into the second of (21) and completing the ζ-integration. It results then that

$$\begin{aligned} H(\xi; \alpha, \lambda) &= H_1(\xi; \alpha)\lambda + H_0(\xi; \alpha) + 0(1) \\ &= \frac{4}{\pi\alpha^2}(\alpha - 2\xi)\lambda + \frac{1}{\pi\alpha}(3\alpha - 4\xi) + o(1) \qquad \text{as } \lambda \to \infty. \end{aligned} \tag{28}$$

Examination of eqns (20) and (28) shows that

$$\phi(\xi; \alpha, \lambda) = \phi_1(\xi; \alpha)\lambda + \phi_0(\xi; \alpha) + o(1) \qquad \text{as } \lambda \to \infty, \tag{29}$$

where $\phi_k (k = 0, 1)$ are the solutions to the integral equations

$$\phi_k(\xi; \alpha) - \int_0^\alpha K(\xi, \eta; \alpha)\phi_k(\eta; \alpha)\,d\eta = H_k(\xi; \alpha) \qquad (0 \leq \xi \leq \alpha). \tag{30}$$

It may be concluded from (29) and (23) that the dimensionless stress intensity factor κ has the asymptotic form

$$\kappa(\alpha, \lambda) = \frac{1}{\sqrt{\alpha}}[\phi_1(0; \alpha)\lambda + \phi_0(0; \alpha) + o(1)] \qquad \text{as } \lambda \to \infty. \tag{31}$$

Finally note from (23), (22) and a physical observation that for any fixed h and l (i.e. λ fixed)

$$\left.\begin{aligned}\lim_{\alpha\to\infty}\kappa(\alpha,\lambda) &= \lim_{\alpha\to\infty}\left[\sqrt{h}\lim_{x\to 0-}\sqrt{-x}\sigma_{xx}(x,-h/2)\right]\\ &= C(\lambda).\end{aligned}\right\} \tag{32}$$

Accordingly, from (31) and (32) there are two constants C_k such that

$$\lim_{\alpha\to\infty}\frac{\phi_k(0;\alpha)}{\sqrt{\alpha}} = C_k \quad (k=1,0). \tag{33}$$

Presentation of other results is postponed until Section 4 where numerical solutions are developed and discussed.

3. STRUCTURAL MODEL BASED UPON A REFINED PLATE THEORY

In this section the double cantilever beam is modeled by two parallel thin plates bonded together along part of their common interface. The structural response of the plate is estimated using a refined plate theory developed in [13]. The assumption of plane strain is retained so that the governing equations for the plate reduce to a system of ordinary differential equations in the independent variable x.

Following the convention of the plate theory [13] the resultant shearing force, V, and bending moment, M, are introduced in addition to the displacements and the stresses. Finally, the bounding surfaces, $z = \pm h/2$, of the plate are assumed free from shearing stress, but subject to normal stresses

$$\sigma_{zz}\left(x,\frac{h}{2}\right) = q(x), \quad \sigma_{zz}\left(x,-\frac{h}{2}\right) = p(x). \tag{34}$$

Due to the plane strain assumption, the displacements† and stresses† in [13] reduce to

$$\left.\begin{aligned}u(x,z) &= \beta(x)z,\\ w(x,z) &= w_0(x) + w_1(x)z + \frac{1}{2}w_2(x)z^2,\\ \sigma_{xx}(x,z) &= \frac{12}{h^3}M(x)z,\\ \tau_{xz}(x,z) &= \frac{3}{2h}V(x)\left[1-\frac{4z^2}{h^2}\right],\\ \sigma_{zz}(x,z) &= \frac{1}{2}[q(x)+p(x)] + \frac{1}{4}[q(x)-p(x)]\left[\frac{3}{2}\frac{z}{h} - \frac{2z^3}{h^3}\right]\end{aligned}\right\} \tag{35}$$

where β, w_0 are the rotation of the normal to the middle plane, the transverse displacement of the middle plane, respectively, while

$$\left.\begin{aligned}w_1(x) &= \frac{1}{2E}[q(x)+p(x)],\\ w_2(x) &= \frac{\mathrm{d}}{\mathrm{d}x}\left[\left(-\frac{9}{7}+\frac{12\nu^2}{5(1-\nu)}\right)\frac{V(x)}{Eh} - \frac{\nu}{1-\nu}\beta(x)\right].\end{aligned}\right\} \tag{36}$$

Further, the moment M, rotation β and shearing force V are related by

$$\left.\begin{aligned}M(x) &= \frac{\mathrm{d}}{\mathrm{d}x}\left[\frac{Eh^3}{12(1-\nu^2)}\beta(x) - \frac{\nu h^2}{10(1-\nu)}V(x)\right],\\ \beta(x) &= -\frac{\mathrm{d}}{\mathrm{d}x}\left[w_0(x)+\frac{h^2}{40}w_2(x)\right] + \frac{12}{5}\frac{1+\nu}{Eh}V(x),\end{aligned}\right\} \tag{37}$$

†See [13] for the results and their derivation for the general case where the assumption of plane strain is dropped.

while M and V satisfy the following system of ordinary differential equations;

$$\frac{\mathrm{d}}{\mathrm{d}x}M(x) = V(x), \quad \frac{\mathrm{d}}{\mathrm{d}x}V(x) + q(x) = 0. \tag{38}$$

Within the framework of the refined plate theory, the loading, constraint and boundary conditions (1) become

$$\left.\begin{aligned} &q(x) = 0 && (-a < x < l),\\ &p(x) = 0 && (0 < x < l),\\ &w(x, -h/2) = 0 && (-a < x < 0),\\ &V(l) = P_0,\ M(l) = 0,\\ &V(-a) = 0,\ M(-a) = 0. \end{aligned}\right\} \tag{39}$$

To facilitate the analysis, divide the original interval $(-a, l)$ into two intervals $(-a, 0)$, $(0, l)$. Continuity conditions at $x = 0$ require that the resultant shearing force V, the bending moment M as well as the rotation and the normalized lateral displacement must all be continuous at that point. Since

$$\left.\begin{aligned} &\frac{12}{h^3}\int_{-h/2}^{h/2} u(x, z)z\,\mathrm{d}z = \beta(x),\\ &\frac{3}{2h}\int_{-h/2}^{h/2} w(x, z)\left(1 - 4\frac{z^2}{h^2}\right)\mathrm{d}z = w_0(x) + \frac{h^2}{40}w_2(x), \end{aligned}\right\} \tag{40}$$

it follows that the end conditions and the continuity conditions for the two intervals are

$$\left.\begin{aligned} &V(-a) = 0,\ M(-a) = 0,\\ &V(0-) = V(0+),\ M(0-) = M(0+),\\ &\beta(0-) = \beta(0+),\\ &w_0(0-) + \frac{h^2}{40}w_2(0-) = w_0(0+) + \frac{h^2}{40}w_2(0+),\\ &V(l) = P_0,\ M(l) = 0. \end{aligned}\right\} \tag{41}$$

After some manipulation of (35)–(37) and the first and the third equations in (39), all of the unknown quantities in the interval $(-a, 0)$ may be expressed in terms of the resultant shear $V(x)$. We list here only those that are needed later:

$$\left.\begin{aligned} p(x) &= \frac{\mathrm{d}}{\mathrm{d}x}V(x),\\ M(x) &= \frac{h^2}{5}\frac{\mathrm{d}V}{\mathrm{d}x} - \frac{265 - 84\nu^2}{8400(1-\nu^2)}h^4\frac{\mathrm{d}^3V}{\mathrm{d}x^3},\\ w_0(x) + \frac{h^2}{40}w_2(x) &= \left[\frac{12}{35} + \frac{3\nu(2+\nu)}{25}\right]\frac{h}{E}\frac{\mathrm{d}V}{\mathrm{d}x}\\ &\quad - \frac{265 - 84\nu^2}{7000}\frac{\nu}{1-\nu}\frac{h^3}{E}\frac{\mathrm{d}^3V}{\mathrm{d}x^3} \qquad (-a < x < 0). \end{aligned}\right\} \tag{42}$$

Further, substitution of $M(x)$ from (42) into the first of (38) leads to the following differential equation for the resultant shear:

$$h^4\frac{\mathrm{d}^4}{\mathrm{d}x^4}V(x) - 1680(1-\nu^2)\gamma h^2\frac{\mathrm{d}^2}{\mathrm{d}x^2}V(x) + 8400(1-\nu^2)\gamma V(x) = 0 \qquad (-a < x < 0), \tag{43}$$

where

$$\gamma = \frac{1}{265 - 84\nu^2}. \tag{44}$$

On the other hand, on the interval $(0, l)$, the quantities $V(x)$, $M(x)$, $w_1(x)$ are readily obtained from (38), (36) and (41):

$$V(x) = P_0, \quad M(x) = P_0(x - l), \quad w_1(x) = 0 \qquad (0 < x < l). \tag{45}$$

In view of the second of (36), the second of (37) and (45), the quantities $w_0(x)$, $w_2(x)$ and $\beta(x)$ must satisfy the relation

$$\left.\begin{aligned} \beta(x) &= -\frac{\mathrm{d}}{\mathrm{d}x}\left[w_0(x) + \frac{h^2}{40}w_2(x)\right] + \frac{12}{5}\frac{1+\nu}{hE}P_0, \\ w_2(x) &= -\frac{\nu}{1-\nu}\frac{\mathrm{d}}{\mathrm{d}x}\beta(x) \qquad (0 < x < l). \end{aligned}\right\} \tag{46}$$

Substitution of β, V, and M from (46) and (45) into the first of (37) then gives

$$\frac{\mathrm{d}^2}{\mathrm{d}x^2}\left[w_0(x) + \frac{h^2}{40}w_2(x)\right] = \frac{12(1-\nu^2)P_0}{Eh^3}(l - x) \qquad (0 < x < l). \tag{47}$$

We next solve eqn (43) for V on the interval $(-a, 0)$ and substitute this into (42) to obtain the corresponding moment M. Satisfaction of the first two conditions in (41) leads to the result

$$\begin{aligned} \frac{V(x)}{P_0} &= A_0\{c\cosh(\hat{c}(x))\sin(\hat{d}(x)) + d\sinh(\hat{c}(x))\cos(\hat{d}(x))\} \\ &\quad + A_3\sinh(\hat{c}(x))\sin(\hat{d}(x)), \qquad (-a < x < 0), \end{aligned} \tag{48}$$

where

$$\hat{c}(x) = \frac{c(x+a)}{h}, \qquad \hat{d}(x) = \frac{d(x+a)}{h}, \tag{49}$$

and c, d are the positive roots of

$$c^2 - d^2 = 840(1-\nu^2)\gamma, \qquad (c^2 + d^2)^2 = 8400(1-\nu)\gamma. \tag{50}$$

The two constants A_0, A_3 in (48) are determined from

$$V(0) = P_0, \qquad M(0) = -P_0 l. \tag{51}$$

In this manner one finds that

$$\left.\begin{aligned} A_0 &= -(c^2 + d^2)\cdot\left\{\frac{l}{h}\sinh\left(\frac{ca}{h}\right)\sin\left(\frac{da}{h}\right) + \frac{c}{c^2+d^2}\cosh\left(\frac{ca}{h}\right)\sin\left(\frac{da}{h}\right)\right. \\ &\quad \left. - \frac{\mathrm{d}}{c^2+d^2}\sinh\left(\frac{ca}{h}\right)\cos\left(\frac{da}{h}\right)\right\}\Big/\Delta, \\ A_3 &= (c^2 + d^2)\cdot\left\{\frac{l}{h}c\cosh\left(\frac{ca}{h}\right)\sin\left(\frac{da}{h}\right) + \frac{l}{h}\mathrm{d}\sinh\left(\frac{ca}{h}\right)\cos\left(\frac{da}{h}\right)\right. \\ &\quad \left. + \sinh\left(\frac{ca}{h}\right)\sin\left(\frac{da}{h}\right)\right\}\Big/\Delta, \end{aligned}\right\} \tag{52}$$

where

$$\Delta = \mathrm{d}^2\sinh^2\left(\frac{ca}{h}\right) - c^2\sin^2\left(\frac{da}{h}\right). \tag{53}$$

The resultant shear V over the interval $(-a, 0)$ is now completely determined as given by (48) and (52) and the remaining quantities on the interval $(-a, 0)$ follow from (42).

Attention is now turned to the determination of the quantities in the interval $(0, l)$. The solution to (47) is given by

$$w_0(x)+\frac{h^2}{40}w_2(x)=\frac{P_0}{E}\left[\bar{A}+\bar{B}\frac{x}{h}+\frac{2(1-\nu^2)}{h^3}(3lx^2-x^3)\right] \tag{54}$$

where $\bar{A}$ and $\bar{B}$ are constants of integration. Substitution from (54) into the first of (46) and subsequent enforcement of the fifth and the sixth equation in (41) yields

$$\begin{aligned}\bar{A}&=\frac{E}{P_0}\left[w_0(0-)+\frac{h^2}{40}w_2(0-)\right],\\ \bar{B}&=\frac{12}{5}(1+\nu)-\frac{Eh}{P_0}\beta(0-).\end{aligned} \tag{55}$$

The right hand side of (55) can be readily expressed in terms of known quantities through the use of (42), the second of (37) and (48). Thus, all the physical quantities in the interval $(0, l)$ are established through (45), (46), (54) together with $\bar{A}$ and $\bar{B}$ in (55).

It is a straightforward matter to obtain an expression for the total strain energy W of the double cantilever specimen. Equation (54) gives the average normal displacement and thus, W is given by

$$\begin{aligned}W&=2\cdot\frac{1}{2}\cdot P_0\cdot\left[w_0(l)+\frac{h^2}{40}w_2(l)\right]\\ &=\frac{P_0^2}{E}\cdot\left[\bar{A}+\bar{B}\cdot\frac{l}{h}+4(1-\nu^2)\frac{l^3}{h^3}\right].\end{aligned} \tag{56}$$

As observed in Section 2, the exact solution to this problem within the framework of two-dimensional elasticity theory exhibits a singular stress field at the crack tip. An approximation to the singular part of the stress field can be determined from the total strain energy (56) upon using the principles of fracture mechanics. For the problem at hand the singular behavior is represented by

$$p(x)=\frac{K_I}{\sqrt{-2\pi x}}+0(1)\qquad \text{as } x\to 0- \tag{57}$$

where K_I is the stress intensity factor. The stress intensity factor is related to the total strain energy of the system[17] by the expression

$$K_I=\left[\frac{E}{1-\nu^2}\frac{\partial w}{\partial l}\right]^{1/2}\quad \text{(fixed force, plane strain)}. \tag{58}$$

Substitution of W from (56) into (58) then yields

$$K_I=2\sqrt{3}\frac{P_0 l}{h^{3/2}}\left\{1+\frac{h^2}{12(1-\nu^2)l^2}\frac{\partial}{\partial(l/h)}\left[\bar{A}+\bar{B}\frac{l}{h}\right]\right\}^{1/2}. \tag{59}$$

Our next objective is to obtain an asymptotic representation of the stress intensity factor valid for large values of $\lambda = l/h$ and $\alpha = a/h$. After tedious calculation based on (55), (42), the second of (37), and (52), we obtain

$$\bar{A}+\bar{B}\lambda=12(1-\nu^2)\eta(\nu)\lambda^2+C_1(\nu)\lambda+C_2(\nu)+0(1/\lambda)\quad \text{as } \lambda\to\infty,\ \alpha\to\infty, \tag{60}$$

where $C_1(\nu)$ and $C_2(\nu)$ are constants, while

$$\eta(\nu)=\frac{c(c^2+d^2)}{5(c^2-d^2)}=\frac{c}{5}\left[\frac{265-84\nu^2}{84(1-\nu^2)}\right]^{1/2} \tag{61}$$

in which c, d are given in (50).

Substituting from (60) into (59) leads to

$$K_I(\alpha,\lambda)=K_I^*(\lambda)+o(1) \qquad \text{as } \lambda\to\infty,\ \alpha\to\infty \tag{62}$$

where the dependence of K_I on α and λ is now explicitly shown and

$$K_I^*(\lambda)=2\sqrt{3}\cdot\frac{P_0\lambda}{\sqrt{h}}\cdot\left[1+\frac{\eta(\nu)}{\lambda}\right]. \tag{63}$$

4. NUMERICAL RESULTS, DISCUSSION

We turn now to the numerical evaluation of the bond stress distribution and to the stress intensity factor furnished by the two alternative models in Sections 2 and 3.

The kernel of the integral eqn (20)—appropriate to the elasticity model—involves an infinite integral F defined by (8). This integral is evaluated by a procedure similar to that employed in [3]. The contribution from the Cauchy type singularities in the kernel K and the right hand member H given by (21) are removed by recognizing the integral

$$\int_0^\alpha \frac{\sqrt{\zeta(\alpha-\zeta)}}{\zeta-\xi}\,d\zeta=\frac{\pi}{2}(\alpha-2\xi) \qquad (0\le\xi\le\alpha). \tag{64}$$

The remaining regular integrals are evaluated numerically. To permit the numerical solution of the integral eqn (20), a uniform partition on the interval $[0,\alpha]$ is introduced and the unknown function approximated by continuous base functions that are linear in each subinterval. The contributions over the first and the last interval are evaluated taking the square root singularities of the kernel into account and the trapezoidal rule is employed for the remainder. In this manner the integral equation is reduced to an approximating system of linear algebraic equations for the values of ϕ at the mesh points. Once ϕ is determined, the bond stress p and the stresses in the adhesive joint are evaluated from (19) and (11).

By means of a somewhat simpler calculation the bond line stress predicted by the refined plate theory can be evaluated from the first of (42), (48) and (52).

Figures 2 and 3 show the variations of the bond stress along the bond line for $l/h=4$ when $a/h=1$ and 3 respectively. In these Figures, the solid curves represent the result appropriate to the elasticity model which is exact within the scope of the two-dimensional theory of plane strain. The dashed curves represent the results based on the refined plate theory, while the dash-dotted curves exhibit those obtained from the singular term in (57) with K_I given by (59).

Even though the case of $a/h=1$ is a severe test for any plate theory, the overall agreement between the two results in Fig. 2 is not too bad. In Fig. 3, the agreement between the exact result and that based on the approximate theory is excellent for $a/h=3$, if the approximate dashed curve is replaced by the dash-dotted curve for the singular term near the origin. Of course, it is to be expected that the plate theory is only applicable when $a/h\gg 1$, $l/h\gg 1$ and these figures indicate this.

Next examine the dependence of the dimensionless stress intensity factor defined by (22), (23) on the parameter λ for various values of α. In Fig. 4, the solid curves represent the results obtained from the integral eqn (20); the dash-dotted curve is the result $1/(\pi\lambda^{1/2})$ which corresponds to the cracked plane. The curves for $\alpha=3$ and 4 almost coalesce to that for $\alpha=5$ and therefore are omitted. The graph reveals an almost linear dependence of κ on $\lambda>0{\cdot}5$ as predicted by (31) and (63).

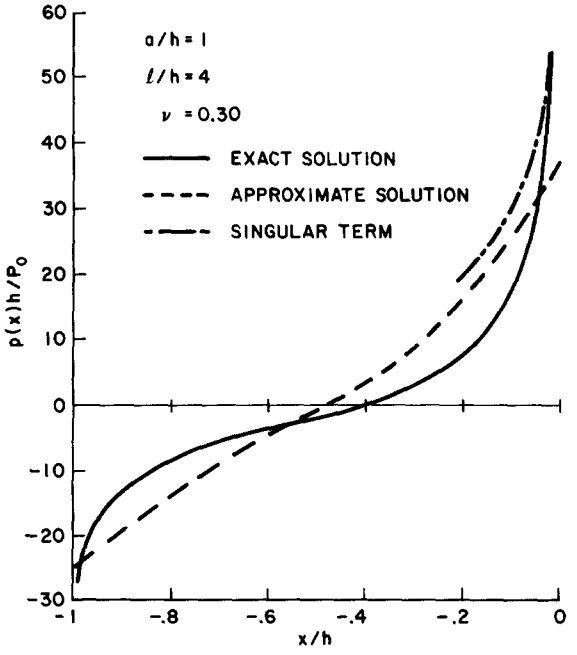

Fig. 2. Variation of bond stress $a/h = 1, l/h = 4$.

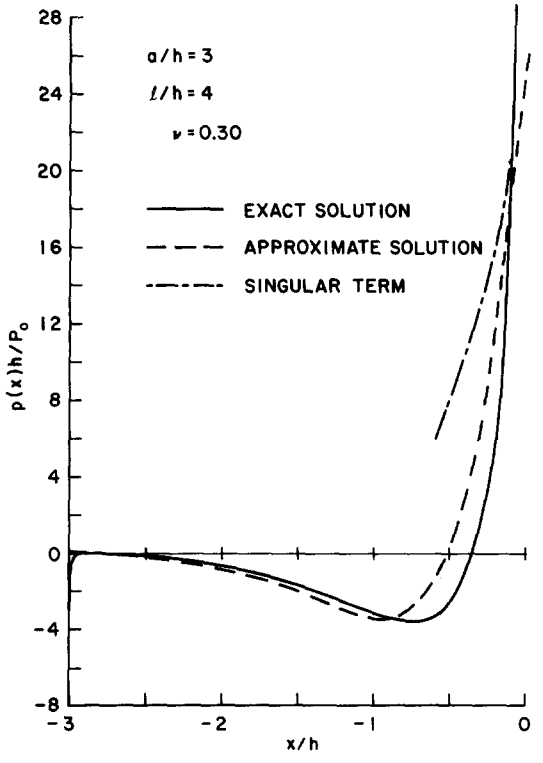

Fig. 3. Variation of bond stress $a/h = 3, l/h = 4$.

From (22), (23), (31) and (33) it results that

$$K_I(\alpha, \lambda) = P_0 \cdot \sqrt{\frac{2\pi}{h}} \cdot \kappa(\alpha, \lambda)$$

$$= \frac{P_0 l}{h^{3/2}} C_1 \left[1 + \frac{C_0}{2C_1} \frac{h}{l}\right] \quad \text{as } \lambda \to \infty, \quad \text{as } \alpha \to \infty, \tag{65}$$

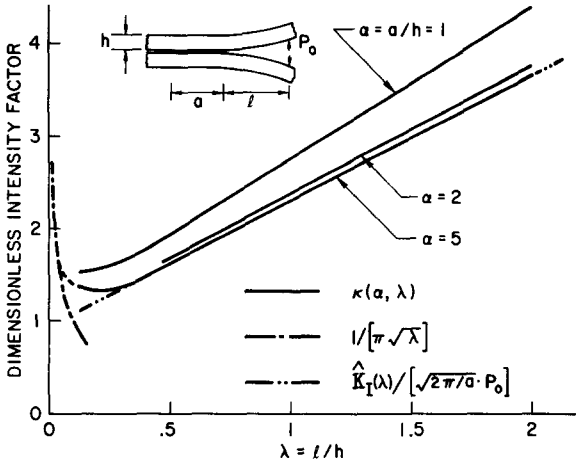

Fig. 4. Dependence of dimensionless stress intensity factor on l/h.

where

$$C_i = 4\sqrt{\pi}\lim_{\alpha\to\infty}\frac{\phi_i(0;\alpha)}{\sqrt{\alpha}} \qquad (i = 1, 0). \tag{66}$$

Numerical solutions of the integral eqn (30) were obtained for $\alpha = 1, 2, 3, 4, 5$ which indicate that $C_1 = 3{\cdot}46$, $C_0 = 4{\cdot}66$. Therefore, eqn (65) becomes

$$K_I(\alpha, \lambda) = 3{\cdot}46\frac{P_0 l}{h^{3/2}}\left[1 + 0{\cdot}675\frac{h}{l}\right] \equiv \hat{K}_I(\lambda) \quad \text{as } \lambda \to \infty, \quad \text{as } \alpha \to \infty \tag{67}$$

where the expression $\hat{K}_I(\lambda)$ has been introduced for this limiting behavior.

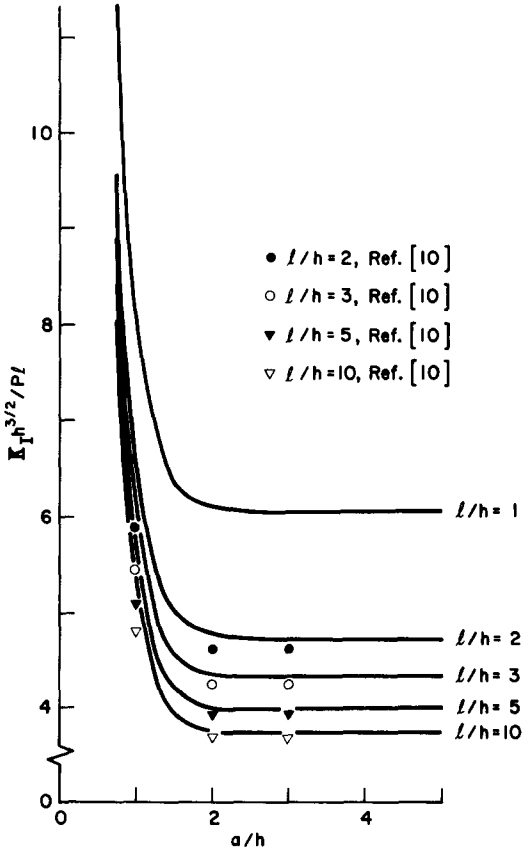

Fig. 5. Dependence of approximate stress intensity factor upon geometry.

This dimensionless counterpart of $\hat{K}_I(\lambda)$ related through $\hat{\kappa} = \hat{K}_I \cdot P_0 \cdot (2h/\pi)^{1/2}$ is shown by dash double dotted curve in Fig. 4. It is apparent from the figure that the stress intensity factor K_I is fairly accurately expressed by $\hat{K}_I$ for $(a/h) > 3$ and $(l/h) > 0{\cdot}5$.

In contrast to K_I in (67), the coefficient of $h/l = 1/\lambda$ in (63) depends upon Poisson's ratio due to the approximate nature of the plate theory. In fact, the coefficient η increases monotonically with ν with the end point values $\eta(0) = 0{\cdot}745$, $\eta(0{\cdot}5) = 0{\cdot}770$.

Even in the most unfavorable case of $\nu = 0{\cdot}5$, the ratio of approximate and "exact" solutions for K are given by

$$\begin{aligned} \hat{K}_I/K_I^* &= 0{\cdot}95 \quad \text{for} \quad l/h = 1, \\ \hat{K}_I/K_I^* &= 0{\cdot}96 \quad\quad\ \ l/h = 2, \\ \hat{K}_I/K_I^* &= 0{\cdot}98 \quad\quad\ \ l/h = 3, \\ \hat{K}_I/K_I^* &= 1 \quad\quad\ \ \text{as} \quad l/h \to \infty. \end{aligned}$$

Thus, the approximate theory in Section 3 gives strikingly accurate stress intensity factors for $a/h > 3$ and $l/h > 2$, the error being less than 4%.

Finally, Fig. 5 presents the normalized stress intensity factors based on the approximate theory ($\nu = 0{\cdot}30$). Numerical results determined by boundary collocation[10] have been plotted as well for purposes of comparison. Compared to the collocation results, the approximate solution appears to lead to a maximum difference of 4% (average of 2%) provided $a/h \geq 2$.

Acknowledgement—This work was supported by the National Science Foundation under Grant GK 30773, at the University of California, Los Angeles.

REFERENCES

1. R. L. Patrick, *Treatise on Adhesion and Adhesives.* Vol. 1, p. 233. Marcel Dekker (1967).
2. R. A. Westmann, Geometrical effects in adhesive joints. *Int. J. Engng Sci.* **13**, 369 (1975).
3. D. J. Chang and R. Muki, Stress distribution in a lap joint under tension-shear. *Int. J. Solids Structures* **10**, 503 (1974).
4. S. K. Chan, I. S. Tuba and W. K. Wilson, On the finite element method in linear fracture mechanics. *Engng Frac. Mech.* **2**, 1 (1970).
5. M. Goland and E. Reissner, The stressses in cemented joints. *J. Appl. Mech.* **11**, 17 (1944).
6. R. W. Cornell, Determination of stresses in cemented lap joints. *J. Appl. Mech.* **20**, 355 (1953).
7. J. L. Lubkin, A theory of adhesive scarf joints. *J. Appl. Mech.* **24**, 255 (1957).
8. J. J. Gilman, *Fracture.* (Edited by B. L. Averback) p. 193. MIT Press, Cambridge (1959).
9. E. J. Ripling, S. Mostovoy and R. L. Patrick, Measuring fracture toughness of adhesive joints. *Material Res. Standards* **4**, 139 (1964).
10. B. Gross and J. E. Srawley, NASA Technical Note D-3295 (1966).
11. J. E. Srawley and B. Gross, Stress intensity factors for crackline loaded edge-crack specimens. *Material Res. Standards* **7**, 155 (1967).
12. S. Mostovoy, P. B. Crosley and E. J. Ripling, Use of crack-line-loaded specimens for measuring plane strain fracture toughness. *J. Materials* **2**, 661 (1967).
13. K. S. Pister and R. A. Westmann, Bending of plates on an elastic foundation. *J. Appl. Mech.* **29**, 369 (1962).
14. R. A. Westmann, Approximate solution of the trouser leg problem. GALCIT SM 64-18, California Institute of Technology, Pasadena, California (June 1964).
15. M. F. Kanninen, An augmented double cantilever beam model for studying crack propagation and arrest. *Int. J. Frac.* **9**, 83 (1973).
16. N. I. Muskhelishvili, *Singular Integral Equations.* Noordhoff, Groningen (1953).
17. G. C. Sih and H. Liebowitz, Mathematical theories of brittle fracture. *Fracture* (Edited by H. Liebowitz) **2**, 104 (1968).
18. P. C. Paris and G. C. Sih, *Symposium on Fracture Toughness Testing and its Application.* STP 381, p. 30, ASTM (1965).